Coupled Systems Mechanics, *Vol. 7, No. 3 (2018) 353-371*
DOI: https://doi.org/10.12989/csm.2018.7.3.353

Application of Wavenumber-TD approach for time harmonic analysis of concrete arch dam-reservoir systems

Vahid Lotfi[*1] and Gerald Zenz[2a]

[1]Department of Civil and Environmental Engineering, Amirkabir University of Technology, Tehran, Iran
[2]Institute of Hydraulic Engineering and Water Resources Management,
Department of Civil Engineering, Graz University of Technology, Graz, Austria

(Received September 20, 2017, Revised October 30, 2017, Accepted December 19, 2017)

Abstract. The Wavenumber or more accurately Wavenumber-FD approach was initially introduced for two-dimensional dynamic analysis of concrete gravity dam-reservoir systems. The technique was formulated in the context of pure finite element programming in frequency domain. Later on, a variation of the method was proposed which was referred to as Wavenumber-TD approach suitable for time domain type of analysis. Recently, it is also shown that Wavenumber-FD approach may be applied for three-dimensional dynamic analysis of concrete arch dam-reservoir systems. In the present study, application of its variation (i.e., Wavenumber-TD approach) is investigated for three-dimensional problems. The method is initially described. Subsequently, the response of idealized Morrow Point arch dam-reservoir system is obtained by this method and its special cases (i.e., two other well-known absorbing conditions) for time harmonic excitation in stream direction. All results for various considered cases are compared against the exact response for models with different values of normalized reservoir length and reservoir base/sidewalls absorptive conditions.

Keywords: concrete arch dams; wavenumber; absorbing boundary conditions; truncation boundary

1. Introduction

It is a well-known fact for dam specialists that dynamic analysis of concrete arch dam-reservoir systems can be carried out rigorously by FE-(FE-HE) method in the frequency domain. This means that the dam is discretized by solid finite elements, while, the reservoir is divided into two parts, a near-field region (usually an irregular shape) in the vicinity of the dam and a far-field part (assuming uniform channel) which extends to infinity in the upstream direction. The former region is discretized by fluid finite elements and the latter part is modeled by a three-dimensional fluid hyper-element (Waas 1972, Hall and Chopra 1983, Fok and Chopra 1986, Tan and Chopra 1995, Lotfi 2004). It is also understood that employing fluid hyper-elements would lead to the exact solution of the problem. However, it is formulated in the frequency domain and its application in this field has led to many especial purpose programs which were demanding from programming

*Corresponding author, Professor, E-mail: vahlotfi@aut.ac.ir
[a]Professor, E-mail: gerald.zenz@tugraz.at

http://www.techno-press.org/?journal=csm&subpage=8 ISSN: 2234-2184 (Print), 2234-2192 (Online)

point of view.

On the other hand, engineers have often tried to solve this problem in the context of pure finite element programming (FE-FE method of analysis). In this approach, an often simplified condition is imposed on the truncation boundary or the upstream face of the near-field water domain. Thus, the fluid hyper-element is actually excluded from the model. Two of these widely used methods are based on Sommerfeld and Sharan (more accurately modified-Sharan condition adjusted for three-dimensional cases) truncation boundary conditions (Sommerfeld 1949, Sharan 1987, Amanabadi and Lotfi 2017). The main advantage of these conditions is that it can be readily used for time domain analysis. Thus, they are also vastly employed in nonlinear seismic analysis of concrete dams.

Of course, there have also been many researches in the last three decades to develop more accurate absorbing boundary conditions to be applied for similar fluid-structure or soil-structure interaction problems. It should be emphasized that many of these studies are actually limited their works to two-dimensional cases. Perfectly matched layer (Berenger 1994, Chew and Weedon 1994, Basu and Chopra 2003, Jiong *et al*. 2009, Zhen *et al*. 2009, Kim and Pasciak 2012, Khazaee and Lotfi 2014a, Khazaee and Lotfi 2014b) and, high-order non-reflecting boundary condition (Higdon 1986, Givoli and Neta 2003, Hagstrom and Warbuton 2004, Givoli *et al*. 2006, Hagstrom *et al*. 2008, Rabinovich 2011, Samii and Lotfi 2012) are among the two main popular groups of methods which researchers have applied in their attempts. It is emphasized that these techniques have become very popular in recent years due to the fact that they could be applied in time domain as well as the frequency domain.

Recently, another technique is also introduced which is referred to as the Wavenumber approach (Lotfi and Samii 2012). The method is simply applying an absorbing boundary condition on the truncation boundary which is referred to as the Wavenumber condition. It is as simple as employing Sommerfeld or Sharan condition on the truncation boundary. Initially, the approach was merely limited to the full reflective reservoir base case and horizontal excitation (Lotfi and Samii 2012). Subsequently, it was modified for the general base condition (Jafari and Lotfi 2017). The Wavenumber approach utilized in these studies were mainly formulated for frequency domain analysis of concrete gravity dam-reservoir systems (i.e., two-dimensional models). Therefore, it may be designated more accurately as Wavenumber-FD technique. Later on, a variation of Wavenumber method was proposed which is referred to as Wavenumber-TD approach (Lotfi and Zenz 2017). The approximation to the original technique improved its realm of application and allowed it to be carried out in time domain as well as frequency domain.

Parallel to the above-mentioned studies, it was also shown that Wavenumber-FD approach may be applied for three-dimensional dynamic analysis of concrete arch dam-reservoir systems (Amanabadi and Lotfi 2017). Therefore, as a next step, it is also interesting now to investigate application of Wavenumber-TD approach for analysis of concrete arch dams. The method is initially described for three-dimensional problems. Subsequently, the response of idealized Morrow Point arch dam-reservoir system is obtained by this condition and its special cases (i.e., Sommerfeld and Sharan truncation boundary alternatives) for time harmonic excitation in stream direction. Six models are investigated which corresponds to different values of normalized reservoir length and reservoir base absorptive conditions. In all considered cases, the results are compared against the exact response (i.e., obtained by the rigorous FE-(FE-HE) type of analysis) to evaluate the effectiveness of the proposed approach (i.e., Wavenumber-TD) in comparison to its special cases.

It should be also emphasized that the present formulation allows one to readily apply it for

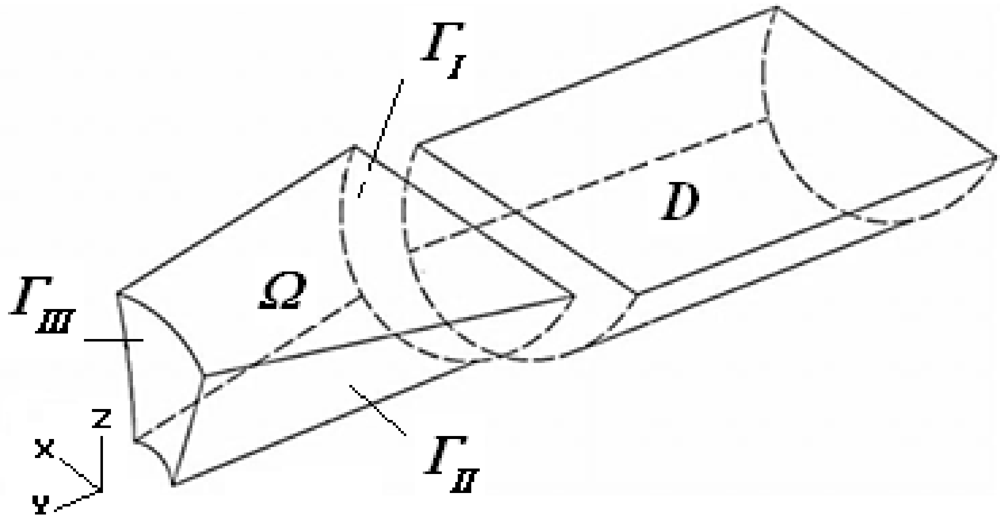

Fig. 1 Schematic view of a typical reservoir (i.e., water domain). The near-field reservoir domain Ω, the truncation boundary Γ_I and the far-field region *D* (excluded in the FE-FE type of analysis)

transient type of analysis (i.e., future study plans). However, it was decided to apply it presently for time harmonic excitation for a better evaluation of error estimate and proof of its effectiveness independent of any specified earthquake excitation.

2. Method of analysis

As mentioned, the analysis technique utilized in this study is based on the FE-FE method, which is applicable for a general concrete arch dam-reservoir system. The coupled equations can be obtained by considering each region separately and then combine the resulting equations.

2.1 Dam body

Concentrating on the structural part, the dynamic behavior of the dam is described by the well-known equation of structural dynamics (Zienkiewicz and Taylor 2000)

$$\mathbf{M}\ddot{\mathbf{r}}+\mathbf{C}\dot{\mathbf{r}}+\mathbf{K}\mathbf{r}=-\tilde{\mathbf{M}}\mathbf{J}\mathbf{a}_g^s+\mathbf{B}^T\mathbf{P} \tag{1}$$

where **M**, **C** and **K** in this relation represent the mass, damping and stiffness matrices of the dam body. Moreover, **r** is the vector of nodal relative displacements, $\tilde{\mathbf{M}}$ is the same as **M** matrix except that no columns are excluded due to restraints, **J** is a matrix with each three rows equal to a 3×3 identity matrix (its columns correspond to a unit cross-canyon, stream and vertical rigid body motion), and $\mathbf{a}^s_g$ denotes the vector of ground accelerations. Furthermore, **B** is a matrix which relates vectors of hydrodynamic pressures (i.e. **P**), and its equivalent nodal forces. It should be also emphasized that $\mathbf{a}^s_g$ denotes the vector of ground accelerations adjusted for stream direction excitation (i.e., the superscript s refers to the stream type of ground motion) which is expressed as below.

$$\mathbf{a}_{\mathrm{g}}^{\mathrm{s}} = \begin{bmatrix} 0 \\ \mathrm{a}_{\mathrm{g}}^{\mathrm{y}} \\ 0 \end{bmatrix} \tag{2}$$

2.2 Water domain

Assuming water to be linearly compressible and neglecting its viscosity, its small irrotational motion (Fig. 1) is governed by the wave equation (Chopra 1967, Chopra, *et al*. 1980) where p is the hydrodynamic pressure and, c is the pressure wave velocity in water.

$$\frac{\partial^2 p}{\partial x^2} + \frac{\partial^2 p}{\partial y^2} + \frac{\partial^2 p}{\partial z^2} - \frac{1}{c^2}\ddot{p} = 0 \qquad \text{(3) in } \boldsymbol{\Omega} \text{ and D}$$

The boundary conditions for reservoir surface and bottom are as follows

$$p = 0 \qquad \text{(4a) on water surface}$$

$$\frac{\partial p}{\partial n} = -\rho\, a_{\mathrm{g}}^{n} - q\,\dot{p} \qquad \text{(4b) at reservoir's bottom/sidewalls}$$

Herein, ρ is the water density and n denotes the outward (with respect to fluid region) perpendicular direction at the reservoir's bottom/sidewalls. Moreover, the admittance or damping coefficient q utilized in the above equation, may be related to a more meaningful wave reflection coefficient $\boldsymbol{\alpha}$ (Fenves and Chopra 1985)

$$\alpha = \frac{1 - q\,c}{1 + q\,c} \tag{5}$$

which is defined as the ratio of the amplitude of reflected hydrodynamic pressure wave to the amplitude of incident pressure wave normal to the reservoir's bottom/sidewalls. For a fully reflective reservoir's bottom/sidewalls condition, $\boldsymbol{\alpha}$ is equal to 1 which leads to q=0.

One can apply the weighted residual approach to obtain the finite element equation of the fluid domain, which may be written as

$$\mathbf{G}^{e}\ddot{\mathbf{P}}^{e} + \mathbf{H}^{e}\mathbf{P}^{e} = \mathbf{R}^{e} \tag{6}$$

With the following definitions

$$\mathbf{G}^{e} = \frac{1}{\rho c^2}\int_{\Omega_e} \mathbf{N}\,\mathbf{N}^{\mathrm{T}}\,\mathrm{d}\Omega \tag{7a}$$

$$\mathbf{H}^{e} = \frac{1}{\rho}\int_{\Omega_e} \left(\mathbf{N}_x\mathbf{N}_x^{\mathrm{T}} + \mathbf{N}_y\mathbf{N}_y^{\mathrm{T}} + \mathbf{N}_z\mathbf{N}_z^{\mathrm{T}}\right)\mathrm{d}\Omega \tag{7b}$$

$$\mathbf{R}^e = \frac{1}{\rho}\int_{\Gamma^e} \mathbf{N}(\partial_n p)\,\mathrm{d}\Gamma^e \tag{7c}$$

With $\mathbf{N}$ being the vector of element's shape functions, and $\mathbf{N}_x$, $\mathbf{N}_y$, $\mathbf{N}_z$ denote its partial derivatives with respect to x, y and z, respectively. It is also worthwhile to emphasize that the superscript (e) states that these matrices are related to element level. The directional derivative $\partial_n p$ in relation (7c), can take three forms on different boundaries of the reservoir (Fig. 1): On the upstream boundary of the reservoir (Γ_{I}): One can apply different absorbing boundary conditions which will be discussed in subsequent sections.

At the reservoir's bottom/sidewalls (Γ_{II}), one can utilize Eq. (4b) as mentioned previously

$$\partial_n p = -\rho a_{\mathrm{g}}^n - q\,\dot{p} \tag{8a}$$

On the dam-reservoir interface (Γ_{III})

$$\partial_n p = -\rho \ddot{u}_n \tag{8b}$$

where $\ddot{u}_n$ is the total acceleration of fluid particles normal to the dam-reservoir interface. It is also noted that there must be compatibility of acceleration between the fluid and solid particles in that direction.

In general, an element may have all three above-mentioned boundary condition types. Thus, one can write $\mathbf{R}^e$ vector as follows

$$\mathbf{R}^e = \mathbf{R}_{\mathrm{I}}^e + \mathbf{R}_{\mathrm{II}}^e + \mathbf{R}_{\mathrm{III}}^e \tag{9}$$

Of course, it is possible that some of these boundary condition types are not applied for a certain element, which that part should be eliminated for that specific element. It is easily shown that one would obtain the following relations by utilizing (8a) and (8b) in (7c), respectively

$$\mathbf{R}_{\mathrm{II}}^e = -\mathbf{B}_{\mathrm{II}}^e\,\mathbf{J}^e\mathbf{a}_{\mathrm{g}}^{\mathrm{s}} - q\mathbf{L}_{\mathrm{II}}^e\,\dot{\mathbf{P}}^e \tag{10a}$$

$$\mathbf{R}_{\mathrm{III}}^e = -\mathbf{B}_{\mathrm{III}}^e(\ddot{\mathbf{r}}^e + \mathbf{J}^e\mathbf{a}_{\mathrm{g}}^s) \tag{10b}$$

With the following definitions

$$\mathbf{B}_{\mathrm{i}}^e = \int_{\Gamma_{\mathrm{i}}^e} \mathbf{N}\mathbf{n}^T\mathbf{N}_{\mathrm{s}}^{\mathrm{T}}\,\mathrm{d}\Gamma^e \quad ;\, \mathrm{i} \in \{\,\mathrm{II},\,\mathrm{III}\} \tag{11a}$$

$$\mathbf{L}_{\mathrm{II}}^e = \frac{1}{\rho}\int_{\Gamma_{\mathrm{II}}^e} \mathbf{N}\,\mathbf{N}^{\mathrm{T}}\mathrm{d}\Gamma^e \tag{11b}$$

Herein, $\mathbf{n}$ represents a unit outward normal vector. Moreover, $\mathbf{N}_{\mathrm{s}}$ is the matrix of adjacent solid element shape functions utilized to interpolate accelerations in cross-canyon, stream and vertical directions. It is worthwhile to mention that from practical point of view, the value of non-zero solid and fluid shape functions are essentially equal on the common fluid-solid interface.

Substituting (10a) and (10b) into (9) will result in

$$\mathbf{R}^e = \mathbf{R}_{\mathrm{I}}^e - q\mathbf{L}_{\mathrm{II}}^e \dot{\mathbf{P}}^e - \mathbf{B}^e \ddot{\mathbf{r}}^e - \mathbf{B}^e \mathbf{J}^e \mathbf{a}_{\mathrm{g}}^{\mathrm{s}} \tag{12}$$

With the following definition

$$\mathbf{B}^e = \mathbf{B}_{\mathrm{II}}^e + \mathbf{B}_{\mathrm{III}}^e \tag{13}$$

It should also be noted that the relative acceleration at boundary Γ_{II} is identically equal to zero. Subsequently, (12) can be substituted in (6) which yields

$$\mathbf{G}^e \ddot{\mathbf{P}}^e + q\mathbf{L}_{\mathrm{II}}^e \dot{\mathbf{P}}^e + \mathbf{H}^e \mathbf{P}^e = \mathbf{R}_{\mathrm{I}}^e(t) - \mathbf{B}^e \ddot{\mathbf{r}}^e - \mathbf{B}^e \mathbf{J}^e \mathbf{a}_{\mathrm{g}}^{\mathrm{s}} \tag{14}$$

Here, $\mathbf{L}_{\mathrm{II}}^e$ is a matrix, which corresponds to the absorption of energy at reservoir's bottom/sidewalls. By assembling the element equations and imposing the free surface condition (4a), one would obtain the overall FE equation of the fluid domain

$$\mathbf{G}\ddot{\mathbf{P}} + q\mathbf{L}_{\mathrm{II}} \dot{\mathbf{P}} + \mathbf{H}\mathbf{P} = \mathbf{R}_{\mathrm{I}} - \mathbf{B}\ddot{\mathbf{r}} - \tilde{\mathbf{B}}\mathbf{J}\mathbf{a}_{\mathrm{g}}^{\mathrm{s}} \tag{15}$$

In this equation, $\mathbf{R}_{\mathrm{I}}$ is obtained by assembling the boundary integrals of Eq. (7c) on Γ_{I}. It should be also noted that $\tilde{\mathbf{B}}$ is the same as $\mathbf{B}$ matrix except that no columns are excluded due to restraints.

2.3 Dam-reservoir system

The necessary equations for both dam and reservoir domains were developed in previous sections. Thus, combining the main relations (15) and (1) would result in the FE equations of the coupled dam-reservoir system in its initial form for the time domain

$$\begin{bmatrix} \mathbf{M} & \mathbf{0} \\ \mathbf{B} & \mathbf{G} \end{bmatrix} \begin{bmatrix} \ddot{\mathbf{r}} \\ \ddot{\mathbf{P}} \end{bmatrix} + \begin{bmatrix} \mathbf{C} & \mathbf{0} \\ \mathbf{0} & q\mathbf{L}_{\mathrm{II}} \end{bmatrix} \begin{bmatrix} \dot{\mathbf{r}} \\ \dot{\mathbf{P}} \end{bmatrix} + \begin{bmatrix} \mathbf{K} & -\mathbf{B}^{\mathrm{T}} \\ \mathbf{0} & \mathbf{H} \end{bmatrix} \begin{bmatrix} \mathbf{r} \\ \mathbf{P} \end{bmatrix} = \begin{bmatrix} -\tilde{\mathbf{M}}\mathbf{J}\mathbf{a}_{\mathrm{g}}^{\mathrm{s}} \\ (-\tilde{\mathbf{B}}\mathbf{J}\mathbf{a}_{\mathrm{g}}^{\mathrm{s}} + \mathbf{R}_{\mathrm{I}}) \end{bmatrix} \tag{16}$$

It is noted from the above equation that vector $\mathbf{R}_{\mathrm{I}}$ still needs to be defined by some appropriate condition. This is related to the truncated boundary Γ_{I} which will be discussed below.

2.4 Modification due to truncation boundary contribution

The effect of truncation boundary condition will be treated in this section. For this purpose, let us now assume that this boundary (i.e., Γ_{I}) is parallel to x-z plane (Fig. 1) and consider a harmonic plane wave with unit amplitude and frequency ω propagating along a direction which makes angles θ_x, θ_y and θ_z with negative x, y and z directions, respectively. This may be written in many different forms such as

$$p = e^{\mathrm{i}(\lambda_x x + k' y + \lambda_z z + \omega t)} \tag{17a}$$

$$p = e^{(\mathrm{i}\,\omega/c)\left[(\cos\theta_x)x + (\cos\theta_y)y + (\cos\theta_z)z + ct\right]} \tag{17b}$$

With the following relations being valid

$$k' = \frac{\omega}{c}\cos\theta_y \tag{18a}$$

$$\lambda_x = \frac{\omega}{c}\cos\theta_x \tag{18b}$$

$$\lambda_z = \frac{\omega}{c}\cos\theta_z \tag{18c}$$

$$k'^2 + \lambda^2 = \frac{\omega^2}{c^2}\ ; \qquad \lambda^2 = {\lambda_x}^2 + {\lambda_z}^2 \tag{18d}$$

It is easily verified that the following condition is appropriate for the truncated boundary based on the assumed traveling wave (i.e., Eq. (17a))

$$\frac{\partial p}{\partial y} - \mathrm{i}\,k'\,p = 0 \tag{19}$$

Employing (19) in (7c), it yields

$$\mathbf{R}_{\mathrm{I}}^{e} = -(\mathrm{i}\,k')\,\mathbf{L}_{\mathrm{I}}^{e}\,\mathbf{P}^{e} \tag{20}$$

With the following definition

$$\mathbf{L}_{\mathrm{I}}^{e} = \frac{1}{\rho}\int_{\Gamma_{\mathrm{I}}^{e}} \mathbf{N}\,\mathbf{N}^{\mathrm{T}}\mathrm{d}\Gamma^{e} \tag{21}$$

Assembling $\mathbf{R}_{\mathrm{I}}^{e}$ for all fluid elements adjacent to truncation boundary leads to

$$\mathbf{R}_{\mathrm{I}} = -(\mathrm{i}k')\mathbf{L}_{\mathrm{I}}\,\mathbf{P} \tag{22a}$$

or by utilizing (18a), one may alternatively write

$$\mathbf{R}_{\mathrm{I}} = -(\frac{\mathrm{i}\omega}{c}\cos\theta_y)\,\mathbf{L}_{\mathrm{I}}\,\mathbf{P} \tag{22b}$$

If the analysis is carried out in the frequency domain, cosθ_y may now be defined in terms of first wavenumber as follows (Amanabadi and Lotfi 2017)

$$\cos\theta_y = \frac{c}{\omega}k_1' \tag{23}$$

Although, relation (23) is easily applied in frequency domain, it cannot be directly employed for an approach which should be applicable for time domain as well as frequency domain analysis. Having this in mind, a suitable form for this aim may now be expressed as

$$\cos\theta_y = \sum_{j=1}^{m} \bar{a}_j (\mathrm{i}\Omega)^{-2(j-1)} + \sum_{j=1}^{n} \bar{b}_j (\mathrm{i}\Omega)^{-2j+1} \tag{24}$$

with the help of dimensionless frequency Ω defined below

$$\Omega = \frac{\omega}{\omega_1^{rs}} \tag{25}$$

In which ω_1^{rs} is the first symmetric natural frequency of the reservoir (i.e., $\omega_1^{rs}=\pi c/\beta_s H$ (Amanabadi and Lotfi 2017)). It is reminded that there are analytical solutions for the natural frequencies of the reservoir in the 2D case. However, this should be obtained numerically in general for three-dimensional cases (Lotfi 2004). It should be also emphasized that the two summations employed in (24) interpolate the real and imaginary parts of $\cos\theta_y$ by utilizing the real and imaginary parts of relation (23), respectively. It is also noted that one may take m, n set of terms for interpolation purposes (i.e., m, n are arbitrary numbers). However, let us adopt the 2, 1 set. That would be

$$\cos\theta_y = \bar{a}_1 + \bar{b}_1 (\mathrm{i}\Omega)^{-1} + \bar{a}_2 (\mathrm{i}\Omega)^{-2} \tag{26}$$

This may now be substituted in (22b) to obtain

$$\mathbf{R}_{\mathrm{I}} = -(a_1(\mathrm{i}\omega) + b_1 + a_2(\mathrm{i}\omega)^{-1})\mathbf{L}_{\mathrm{I}}\,\mathbf{P} \tag{27}$$

With the following definitions for the employed factors

$$a_1 = \frac{\bar{a}_1}{c}\ ;\ b_1 = \frac{\bar{b}_1(\omega_1^{rs})}{c}\ ;\ a_2 = \frac{\bar{a}_2(\omega_1^{rs})^2}{c} \tag{28}$$

Eq. (27) may alternatively be written in time domain as

$$\mathbf{R}_{\mathrm{I}} = -(a_1\mathbf{L}_{\mathrm{I}}\,\dot{\mathbf{P}} + b_1\mathbf{L}_{\mathrm{I}}\,\mathbf{P} + a_2\mathbf{L}_{\mathrm{I}}\,\Phi_1) \tag{29a}$$

In which

$$\dot{\Phi}_1 = \mathbf{P} \tag{29b}$$

Substituting (29a) in (16) and combining it with a third matrix equation obtained through multiplying (29b) by $a_2\mathbf{L}_{\mathrm{I}}$ would lead to the FE equations of the coupled dam-reservoir system in its final form suitable for time domain analysis

$$\begin{bmatrix} \mathbf{M} & \mathbf{0} & \mathbf{0} \\ \mathbf{B} & \mathbf{G} & \mathbf{0} \\ \mathbf{0} & \mathbf{0} & \mathbf{0} \end{bmatrix}\begin{bmatrix} \ddot{\mathbf{r}} \\ \ddot{\mathbf{P}} \\ \ddot{\Phi}_1 \end{bmatrix} + \begin{bmatrix} \mathbf{C} & \mathbf{0} & \mathbf{0} \\ \mathbf{0} & (q\mathbf{L}_{\mathrm{II}} + a_1\mathbf{L}_{\mathrm{I}}) & \mathbf{0} \\ \mathbf{0} & \mathbf{0} & -a_2\mathbf{L}_{\mathrm{I}} \end{bmatrix}\begin{bmatrix} \dot{\mathbf{r}} \\ \dot{\mathbf{P}} \\ \dot{\Phi}_1 \end{bmatrix} + \begin{bmatrix} \mathbf{K} & -\mathbf{B}^{\mathrm{T}} & \mathbf{0} \\ \mathbf{0} & (\mathbf{H} + b_1\mathbf{L}_{\mathrm{I}}) & a_2\mathbf{L}_{\mathrm{I}} \\ \mathbf{0} & a_2\mathbf{L}_{\mathrm{I}} & \mathbf{0} \end{bmatrix}\begin{bmatrix} \mathbf{r} \\ \mathbf{P} \\ \Phi_1 \end{bmatrix}$$
$$= \begin{bmatrix} -\tilde{\mathbf{M}}\,\mathbf{J}\,\mathbf{a}_{\mathrm{g}}^{\mathrm{s}} \\ -\tilde{\mathbf{B}}\,\mathbf{J}\,\mathbf{a}_{\mathrm{g}}^{\mathrm{s}} \\ \mathbf{0} \end{bmatrix} \tag{30}$$

This may be simplified in writing by defining few auxiliary matrices. It is expressed as

$$\begin{bmatrix} \mathbf{M} & \mathbf{0} \\ \bar{\mathbf{B}} & \bar{\mathbf{G}} \end{bmatrix} \begin{bmatrix} \ddot{\mathbf{r}} \\ \ddot{\bar{\mathbf{P}}} \end{bmatrix} + \begin{bmatrix} \mathbf{C} & \mathbf{0} \\ \mathbf{0} & \bar{\mathbf{L}} \end{bmatrix} \begin{bmatrix} \dot{\mathbf{r}} \\ \dot{\bar{\mathbf{P}}} \end{bmatrix} + \begin{bmatrix} \mathbf{K} & -\bar{\mathbf{B}}^{\mathrm{T}} \\ \mathbf{0} & \bar{\mathbf{H}} \end{bmatrix} \begin{bmatrix} \mathbf{r} \\ \bar{\mathbf{P}} \end{bmatrix} = \begin{bmatrix} -\tilde{\mathbf{M}}\,\mathbf{J}\,\mathbf{a}_{\mathrm{g}}^{\mathrm{s}} \\ -\bar{\bar{\mathbf{B}}}\,\mathbf{J}\,\mathbf{a}_{\mathrm{g}}^{\mathrm{s}} \end{bmatrix} \tag{31}$$

Auxiliary matrices with bar signs over them are easily determined by comparing relations (30) and (31). Moreover, the following definition for $\bar{\mathbf{P}}$ vector is utilized

$$\bar{\mathbf{P}} = \begin{bmatrix} \mathbf{P} \\ \Phi_1 \end{bmatrix} \tag{32}$$

It is now apparent that the proposed approach is suitable for transient analysis. However, let us simplify this relation for time harmonic analyses, which is the scope of present study. Under these circumstances, one may write (31) as follows

$$\begin{bmatrix} -\omega^2\mathbf{M} + (1+2\beta\mathrm{i})\mathbf{K} & -\bar{\mathbf{B}}^{\mathrm{T}} \\ -\bar{\mathbf{B}} & \omega^{-2}(-\omega^2\bar{\mathbf{G}} + \mathrm{i}\omega\bar{\mathbf{L}} + \bar{\mathbf{H}}) \end{bmatrix} \begin{Bmatrix} \mathbf{r} \\ \bar{\mathbf{P}} \end{Bmatrix} = \begin{Bmatrix} -\tilde{\mathbf{M}}\,\mathbf{J}\,\mathbf{a}_{\mathrm{g}}^{\mathrm{s}} \\ \omega^{-2}(-\bar{\bar{\mathbf{B}}}\,\mathbf{J}\,\mathbf{a}_{\mathrm{g}}^{\mathrm{s}}) \end{Bmatrix} \tag{33}$$

In this relation, it is assumed that the damping matrix of the dam is of hysteretic type. This means

$$\mathbf{C} = (2\beta/\omega)\mathbf{K} \tag{34}$$

It is also noticed that the lower matrix equation of (33) is multiplied by ω^{-2} in this process to obtain a symmetric dynamic stiffness matrix for the dam-reservoir system.

2.5 Different options for defining coefficients $\bar{a}_j$ and $\bar{b}_j$

It was mentioned that a total of three coefficients (i.e., $\bar{a}_1$, $\bar{b}_1$ and $\bar{a}_2$) are adopted for the present study. However, let us first discuss some special cases which are considered as the subset of the present approach and consider the general case subsequently.

Obviously, one may define these coefficients directly. For instance, assuming the first coefficient as 1 and taking the other two as 0 would lead to the Sommerfeld B.C. While, selecting the first two terms as 1 and the last one as 0 yields the well-known Sharan B.C. as listed in Table 2.1.

Table 2.1 Definitions of required coefficients for two well-known methods

Truncation B.C.	$\bar{a}_1$	$\bar{b}_1$	$\bar{a}_2$
Sommerfeld	1	0	0
Sharan	1	1	0

The alternative is to define these coefficients indirectly. In this case, certain normalized frequencies are specified which corresponds to the points that matching occurs between the interpolating relation and the actual function. For the present Wavenumber (i.e., Wavenumber-TD) condition, this strategy is utilized. In this case, all three coefficients may have non-zero values and they are defined through interpolation means by utilizing relations (23) and (24) as mentioned above. Therefore, a set of normalized frequencies are employed (i.e., Ω_1^R, Ω_2^R and Ω_1^I) for interpolating real and imaginary parts of $\cos\theta_y$. For the present study, these normalized frequencies are selected as listed in Table 2.2 and the resulting computed coefficients are also provided in that Table for two values of $\boldsymbol{\alpha}$ (i.e., reservoir bottom/sidewalls reflection coefficient). These are employed in the analyses carried out and discussed in subsequent sections.

Table 2.2 Definitions of required coefficients for Wavenumber-TD approach

$\boldsymbol{\alpha}$	Ω_1^R	Ω_2^R	$\bar{a}_1$	$\bar{a}_2$	Ω_1^I	$\bar{b}_1$
1.00	0.91	3.0	1.038	0.860	0.91	0.415
0.85	0.91	3.0	1.017	0.685	0.91	0.451

3. Modeling and basic parameters

The introduced methodology is employed to analyze an idealized dam-reservoir system. The details about modeling aspects such as discretization, basic parameters and the assumptions adopted are summarized in this section.

3.1 Models

An idealized symmetric model of Morrow Point arch dam on rigid foundation is considered.
The geometry of the dam may be found in the Reference (Hall and Chopra 1983). The dam is discretized by 40 isoparametric 20-node solid finite element (Fig. 2(a)).

As for the water domain, two strategies are adopted (Figs. 2(b) and 2(c)). For the FE-FE method of analysis which is our main procedure, only the reservoir near-field is discretized and the absorbing boundary condition is employed on the upstream truncation boundary according to different alternatives discussed. The length of this near-field region is denoted by L and water depth is referred to as H. Three normalized reservoir lengths are considered. These are in particular the L/H values of 0.2, 1 and 3 which represent low, moderate and high reservoir lengths (the first two cases are shown in Fig. 2(b)). This region is discretized by 80, 200 and 520 isoparametric 20-node fluid finite elements for three above-mentioned L/H values, respectively.

For the FE-(FE-HE) method of analysis, the reservoir domain is divided into two regions. The near-field region is discretized by fluid finite elements, and the far-field is treated by a fluid hyper-element (Fig. 2(c)). Of course, it should be emphasized that this option is merely utilized to obtain the exact solution (Lotfi 2004). Moreover, it is well-known that the results are not sensitive in this case to the length of the reservoir near-field region or L/H value.

3.2 Basic parameters

The dam body is assumed to be homogeneous and isotropic with linearly viscoelastic properties for mass concrete.

Elastic modulus (E_d)	=27.5 GPa
Poison’s ratio	=0.02
Unit weight	=24.8 kN/m^3
Hysteretic damping factor (β_d)	=0.05

The impounded water is taken as inviscid and compressible fluid with unit weight equal to 9.81 kN/m^3, and pressure wave velocity c=1440 m/sec.

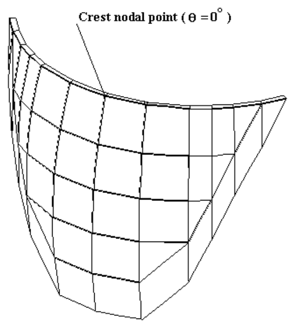

(a) Dam body

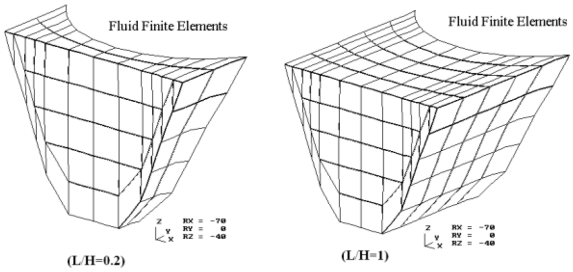

(b) Water domain for FE-FE models of L/H=0.2 and 1

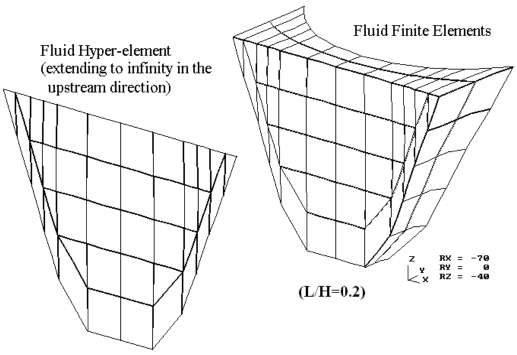

(c) Water domain for FE-(FE-HE) model (fluid finite elements (L/H=0.2), and the fluid hyper-element)

Fig. 2 Discretization of dam-reservoir system

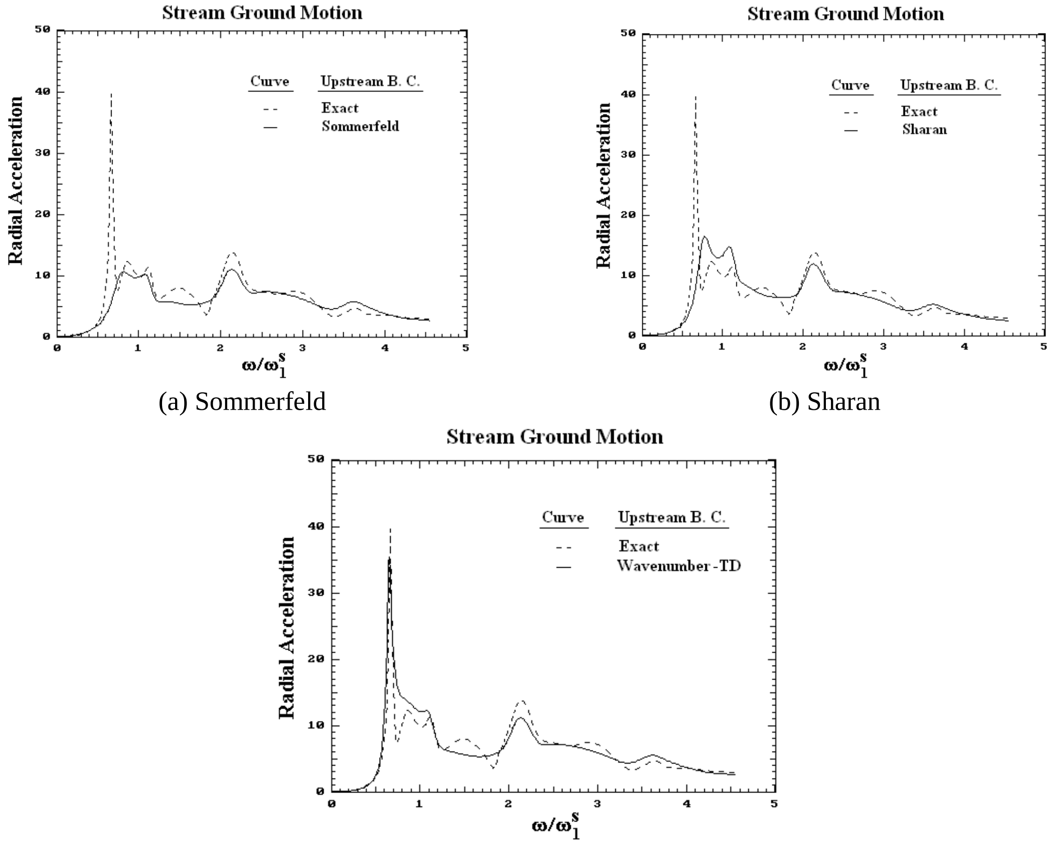

(a) Sommerfeld (b) Sharan

(c) Wavenumber-TD

Fig. 3 Radial acceleration at dam crest due to stream ground motion for different absorbing boundary condition alternatives (L/H=0.2, α=1)

4. Results

It should be emphasized that all results presented herein, are obtained by the FE-FE method discussed, under different absorbing conditions applied on the truncation boundary. The only exception is for what is referred to as the exact response. That especial case is carried out by the FE-(FE-HE) analysis technique (Lotfi 2004).

The initial part of the study is focused on full reflective reservoir base condition (i.e., α=1). Three models are considered with different values of reservoir lengths. These may be referred to as low, moderate and high normalized reservoir lengths (i.e., L/H=0.2, 1 and 3). For each model, three different truncation boundary absorbing conditions are examined. In particular, these are Sommerfeld, Sharan and Wavenumber-TD cases. Subsequently, three other models are evaluated, which are similar to the first three models. However, the reservoir base/sidewalls condition is absorptive in those models (i.e., α=0.85).

The transfer function for the radial acceleration at dam crest (i.e., corresponding to θ =0 (Fig. 2a)) with respect to stream ground acceleration, are presented in Figs. 3-8 for these six models. It is noted that response in each case is plotted versus the dimensionless frequency.

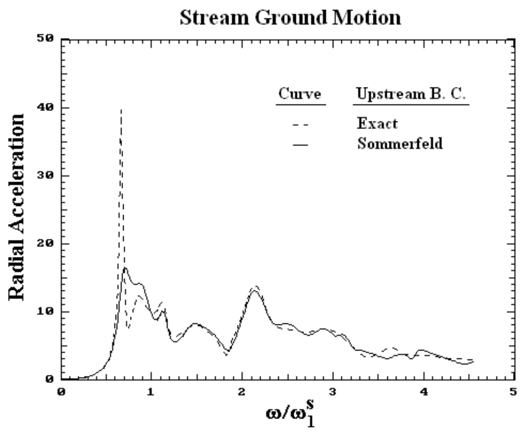

(a) Sommerfeld

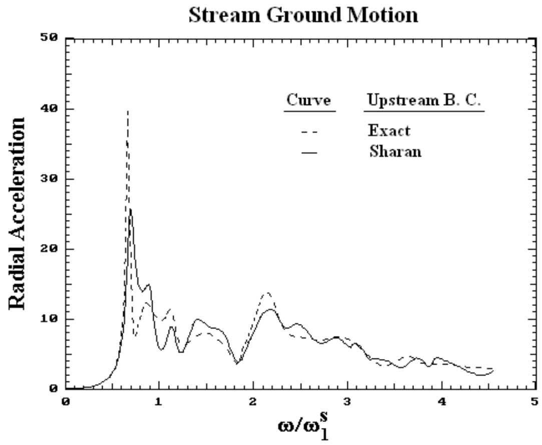

(b) Sharan

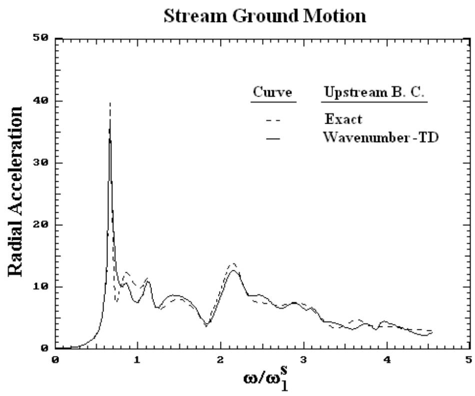

(c) Wavenumber-TD

Fig. 4 Radial acceleration at dam crest due to stream ground motion for different absorbing boundary condition alternatives (L/H=1, $\boldsymbol{\alpha}$=1)

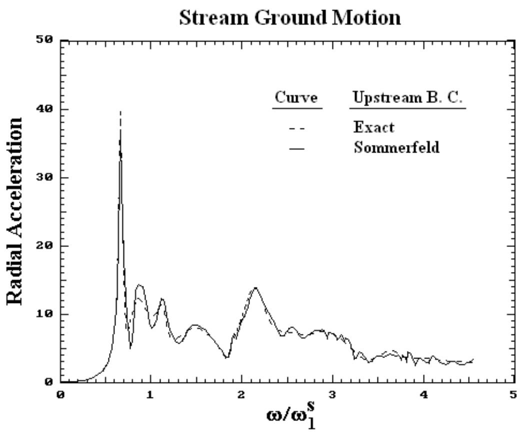

(a) Sommerfeld

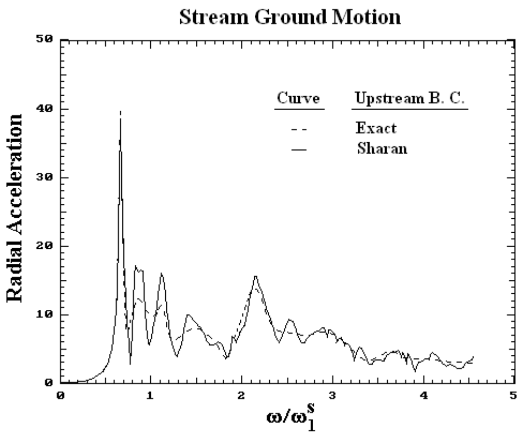

(b) Sharan

Fig. 5 Radial acceleration at dam crest due to stream ground motion for different absorbing boundary condition alternatives (L/H=3, $\boldsymbol{\alpha}$=1)

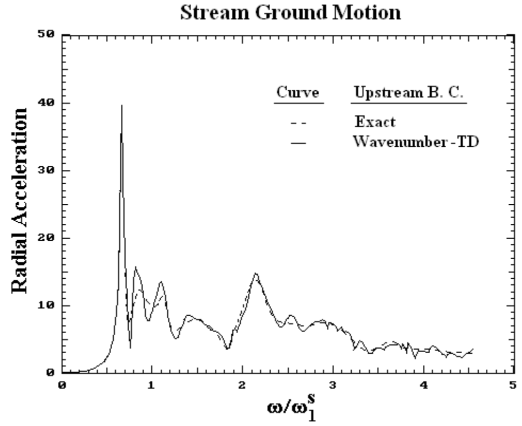

(c) Wavenumber-TD

Fig. 5 Continued

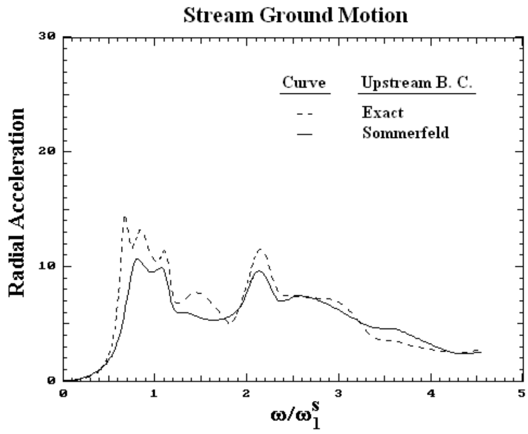

(a) Sommerfeld

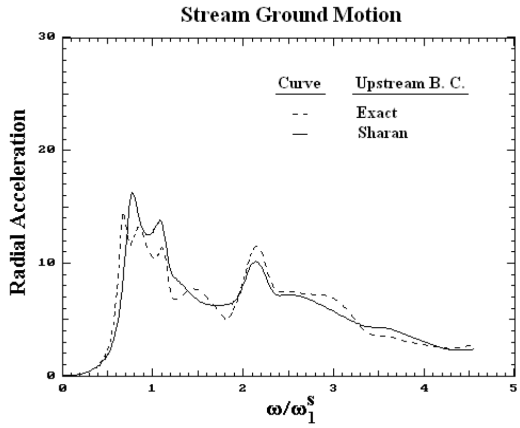

(b) Sharan

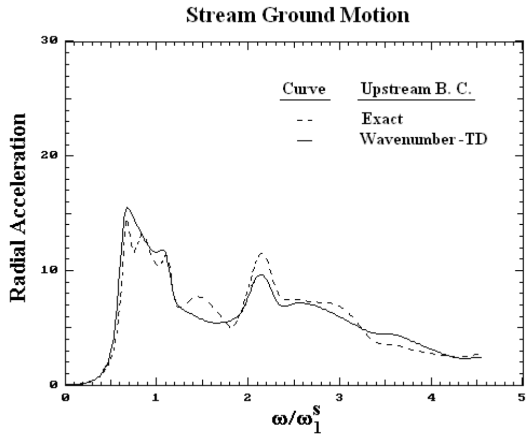

(c) Wavenumber-TD

Fig. 6 Radial acceleration at dam crest due to stream ground motion for different absorbing boundary condition alternatives (L/H=0.2, α=0.85)

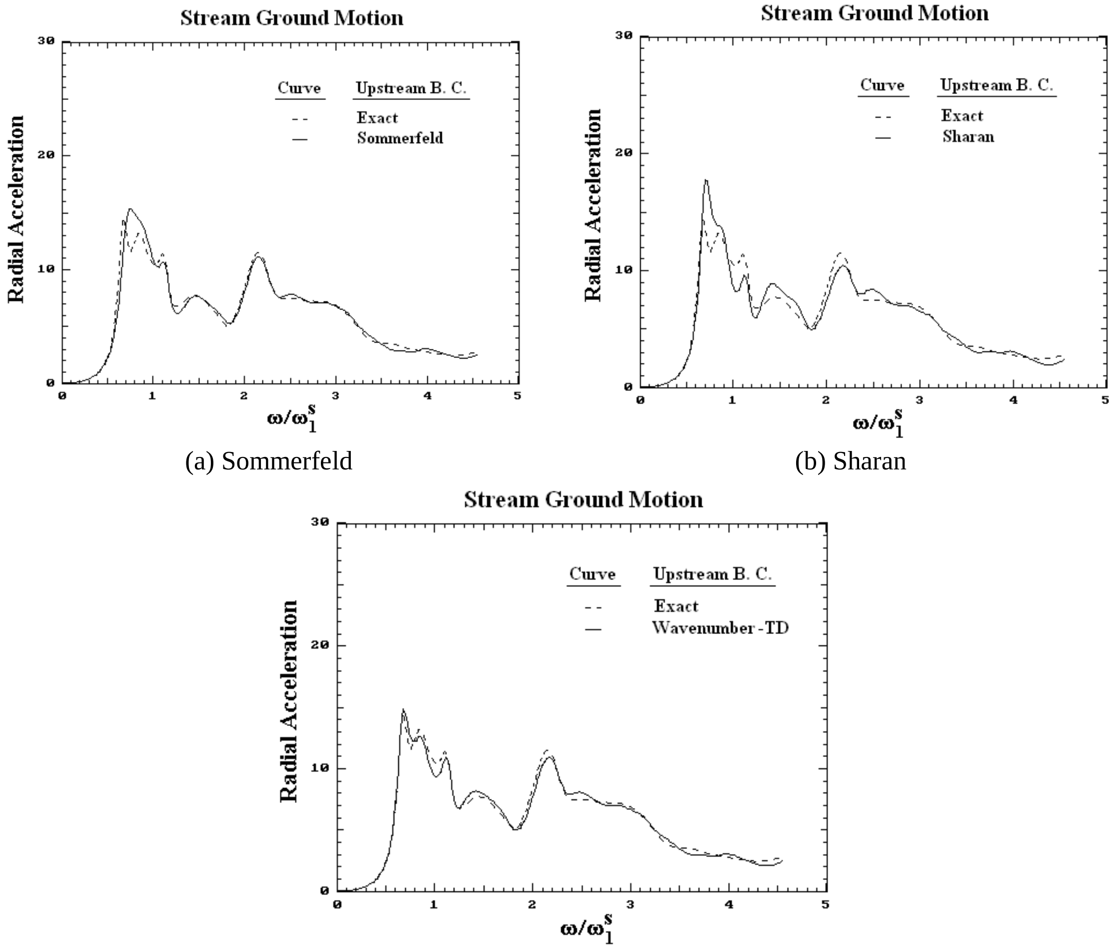

(a) Sommerfeld

(b) Sharan

(c) Wavenumber-TD

Fig. 7 Radial acceleration at dam crest due to stream ground motion for different absorbing boundary condition alternatives (L/H=1, α=0.85)

The normalization of excitation frequency is carried out with respect to $\omega_1{}^S$, which is defined as the fundamental frequency of the dam on rigid foundation with empty reservoir for a symmetric mode. Moreover, it is noticed that all cases are compared with its corresponding exact response.

Let us first consider the initial three models which relates to the full reflective reservoir base/sidewalls condition (i.e., α=1). The responses are plotted in Figs. 3-5. For the low reservoir length model (Fig. 3), it is observed that there are significant errors at the fundamental frequency of the system for the Sommerfeld and Sharan truncation boundary conditions. While, the Wavenumber-TD response is behaving relatively well even under these challenging circumstances (i.e., L/H=0.2 and α=1). It is also important to notice that the fundamental natural frequency of the system is captured accurately for the Wavenumber-TD case, while this is not the case for the other two alternatives. Although, accuracy is slightly improved, similar observations are also valid for the moderate reservoir length model (i.e., L/H=1) as what was asserted for the low reservoir length (Fig. 4 versus Fig. 3). For the high reservoir length model (i.e., L/H=3), responses for all three

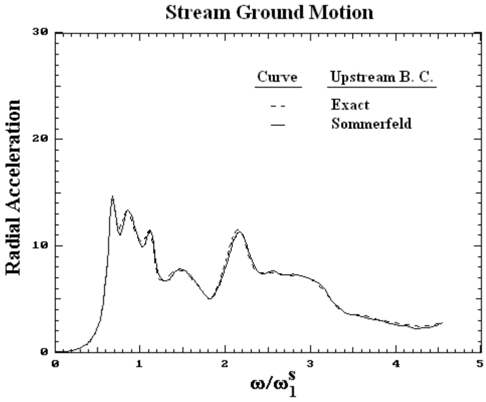

(a) Sommerfeld

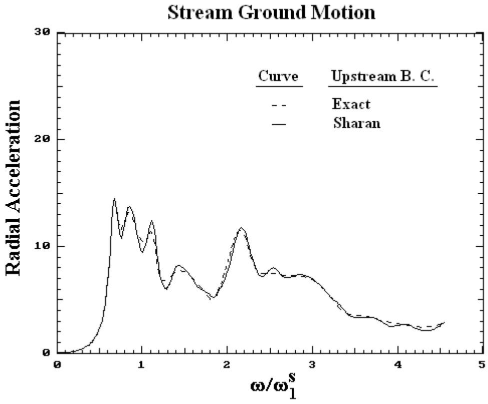

(b) Sharan

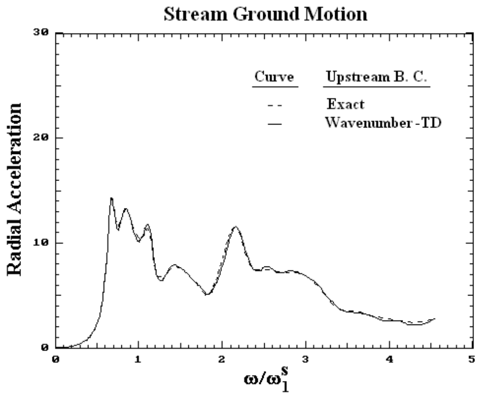

(c) Wavenumber-TD

Fig. 8 Radial acceleration at dam crest due to stream ground motion for different absorbing boundary condition alternatives (L/H=3, α=0.85)

truncation boundary alternatives are acceptable (Fig. 5). Of course, the accuracy of the response at the fundamental frequency of the system (i.e., precision on magnitude of the first major peak) seems to be still highest for Wavenumber-TD alternative and least for the Sommerfeld condition case. The other interesting observation for this high reservoir length model is that some kind of noise or distortion is noticed in the response of Wavenumber-TD case especially for higher frequencies similar to other two alternatives. Something that did not existed on the original Wavenumber truncation condition introduced merely for frequency domain analysis which may be designated as Wavenumber-FD truncation condition (Lotfi and Samii 2012). This oscillatory behavior is originated due to the fact that approximate Wavenumber approach is employed as the basis of wavenumber-TD condition. In other words, one is utilizing first wavenumber for the whole frequency range, while various wavenumbers were employed for different frequency regions in the original Wavenumber approach. Of course, it must be mentioned that one generally expects that these oscillatory noise or distortion diminish as the degree of reservoir base/sidewalls absorption increases.

Subsequently, the results for the other three models are presented (Figs. 6-8). For the low reservoir length model (Fig. 6), it is observed that there is still significant error at the fundamental frequency of the system for the Sommerfeld truncation boundary condition.

Moreover, the fundamental natural frequency of the system is not captured accurately for both Sommerfeld and Sharan truncation boundary conditions. While, the Wavenumber-TD response is behaving very well. This is noticeable for magnitude of the peak at the fundamental frequency of the system and the actual occurrence of that natural frequency. As for the moderate reservoir length model (Fig. 7), it is observed that there is significant error at the fundamental frequency of the system for the Sharan truncation boundary condition. However, response for the Sommerfeld alternative has been improved. It may be asserted that there is now mainly error as far as the fundamental frequency of the system not the corresponding peak of the response. The Wavenumber-TD response is behaving well under these circumstances. In regard to the last model results (Fig. 8), it is observed that all three truncation boundary condition alternatives are now behaving very well. It is worthwhile to mention that as expected, oscillatory noise or distortion is now diminished for all three truncation boundary condition alternatives due to reservoir base/sidewalls absorption.

Finally, percentage of error at the fundamental frequency of the system is also calculated and listed in Table 4.1 for all different cases of six considered models for quantitative evaluation of the amount of error involved in each case.

Overall, it may be concluded that Sommerfeld and Sharan truncation boundary conditions should not be utilized for models with low and moderate normalized reservoir lengths for both full reflective and absorptive reservoir base/sidewalls conditions. In other words, it is merely appropriate for high normalized reservoir lengths. Of course, in moderate normalized reservoir lengths, this assertion for the absorptive case is not deemed as strong as for the full reflective case, especially for the Sommerfeld truncation boundary condition. It should be emphasized that the above-mentioned conclusion is based on considering both error at the first major peak of the response and the accuracy on capturing correct fundamental natural frequency of the system.

Furthermore, it is noticed that Wavenumber-TD condition has produced acceptable results under all different circumstances as well as the most challenging case of low reservoir length and full reflective base condition (i.e., L/H=0.2 and α =1).

Table 4.1 Percentage of error at the fundamental frequency of the system for different cases of six considered models

Model	$\boldsymbol{\alpha}$	L/H	Sommerfeld	Sharan	Wavenumber-TD
1		0.2	73.1	58.4	11.8
2	1.00	1.0	58.6	35.6	7.1
3		3.0	9.3	4.9	1.2
4		0.2	26.4	12.4	7.0
5	0.85	1.0	5.9	22.6	2.3
6		3.0	1.0	0.3	1.2

5. Conclusions

The proposed formulation based on FE-FE procedure for dynamic analysis of concrete arch dam-reservoir systems, was described in great details. Moreover, several options were discussed for imposing a local type of absorbing condition on the truncation boundary of the water domain.

A special purpose finite element program was enhanced for this investigation. Thereafter, the response of idealized Morrow Point arch dam was studied due to stream ground motion for different alternatives employed as absorbing boundary condition. The main approach which was emphasized and proposed in this study is referred to as the Wavenumber-TD approach. It is also shown that the other two considered alternatives (i.e., Sommerfeld and Sharan conditions) may be considered as special cases of the Wavenumber-TD condition. Overall, the main conclusions obtained by the present study can be listed as follows:

• Sommerfeld and Sharan truncation boundary conditions should not be utilized for models with low and moderate normalized reservoir lengths for both full reflective and absorptive reservoir base/sidewalls conditions. In other words, it is merely appropriate for high normalized reservoir lengths. Of course, in moderate normalized reservoir lengths, this assertion for the absorptive case is not deemed as strong as for the full reflective case, especially for the Sommerfeld truncation boundary condition. It should be emphasized that the above-mentioned conclusion is based on considering both error at the first major peak of the response and the accuracy on capturing correct fundamental natural frequency of the system.

• Wavenumber-TD truncation boundary condition has produced acceptable results under all different circumstances as well as the most challenging case of low reservoir length and full reflective base/sidewalls condition (i.e., L/H=0.2 and α=1).

• Finally, it should be emphasized that Wavenumber-TD approach, based on FE-FE method of analysis, is extremely efficient in comparison with the well-known FE-(FE-HE) method. This is due to the fact that in general for absorptive reservoir base/sidewalls condition (i.e., $\alpha \neq 1$), one has to solve an eigenvalue problem for each frequency of excitation in the latter technique to define the necessary matrices for 3D fluid hyper-element. While, one is dealing with a frequency independent matrix $\mathbf{L}_I$ in the former case. Of course, the real advantages of this technique would be more apparent when one employs Wavenumber-TD condition for nonlinear dynamic analysis of concrete dam-reservoir systems which is the plan for future studies. It is well-known that 3D fluid hyper-element cannot be utilized for those type of analyses since it is formulated in the frequency domain.

References

Amanabadi, J. and Lotfi, V. (2017), “Dynamic analysis of three-dimensional dam-reservoir systems by Wavenumber approach in the frequency domain”, *J. Hydrodyn*., Under Review.

Basu, U. and Chopra, A.K. (2003), “Perfectly matched layers for time-harmonic elastodynamics of unbounded domains: Theory and finite-element implementation”, *Comput. Meth. Appl. Mech. Eng*., **192**(11-12), 1337-1375.

Berenger, J.P. (1994), “A perfectly matched layer for the absorption of electromagnetic waves”, *J. Comput. Phys*., **114** (2), 185-200.

Chew, W.C. and Weedon, W.H. (1994), “A 3D perfectly matched medium from modified Maxwell’s equations with stretched coordinates”, *Microw. Opt. Techn. Let*., **7**(13), 599-604.

Chopra, A.K. (1967), “Hydrodynamic pressure on dams during earthquake”, *J. Eng. Mech.-ASCE*, **93**(6), 205-223.

Chopra, A.K., Chakrabarti, P. and Gupta, S. (1980), *Earthquake Response of Concrete Gravity Dams Including Hydrodynamic and Foundation Interaction Effects*, Report No. EERC-80/01, Earthquake Engineering Research Center, University of California, Berkeley, U.S.A.

Fenves, G. and Chopra, A.K. (1985), “Effects of reservoir bottom absorption and dam-water-foundation

interaction on frequency response functions for concrete gravity dams", *Earthq. Eng. Struct. D.*, **13**(1), 13-31.
Fok, K.-L. and Chopra, A.K. (1986), "Frequency response functions for arch dams: hydrodynamic and foundation flexibility effects", *Earthquake Eng. Struct. Dyn.*, **14**(5), 769-795.
Givoli, D. and Neta, B. (2003), "High order non-reflecting boundary scheme for time-dependent waves", *J. Comput. Phys.*, **186**(1), 24-46.
Givoli, D., Hagstrom, T. and Patlashenko, I. (2006), "Finite-element formulation with high-order absorbing conditions for time-dependent waves", *Comput. Meth. Appl. M.*, **195**(29-32), 3666-3690.
Hagstrom, T. and Warburton, T. (2004), "A new auxiliary variable formulation of high order local radiation boundary condition: corner compatibility conditions and extensions to first-order systems", *Wave Motion*, **39**(4), 327-338.
Hagstrom, T., Mar-Or, A. and Givoli, D. (2008), "High-order local absorbing conditions for the wave equation: extensions and improvements", *J. Comput. Phys.*, **227**(6), 3322-3357.
Hall, J.F. and Chopra, A.K. (1983), "Dynamic analysis of arch dams including hydrodynamic effects", *J. Eng. Mech. Div.*, **109**(1), 149-163.
Higdon, R.L. (1986), "Absorbing boundary conditions for difference approximations to the multi-dimensional wave equation", *Math. Comput.*, **47**(176), 437-459.
Jafari, M. and Lotfi, V. (2017), "Dynamic analysis of concrete gravity dam-reservoir systems by Wavenumber approach for the general reservoir base condition", Submitted to the International Journal of Science and Technology (Scientia Iranica), Accepted.
Jiong, L., Jian-wei, M. and Hui-zhu, Y (2009), "The study of perfectly matched layer absorbing boundaries for SH wave fields", *Appl. Geophys.*, **6**(3), 267-274.
Khazaee, A. and Lotfi, V. (2014a), "Application of perfectly matched layers in the transient analysis of dam-reservoir systems", *J. Soil Dynam. Earthq. Eng.*, **60**(1), 51-68.
Khazaee, A. and Lotfi, V. (2014b), "Time harmonic analysis of dam-foundation systems by perfectly matched layers", *J. Struct. Eng. Mech.*, **50**(3), 349-364.
Kim, S. and Pasciak, J.E. (2012), "Analysis of cartesian PML approximation to acoustic scattering problems in R2", *Wave Mot.*, **49**, 238-257.
Lotfi, V. (2004), "Direct frequency domain analysis of concrete arch dams based on FE-(FE-HE)-BE technique", *J. Comp. Concrete*, **1**(3), 285-302.
Lotfi, V. and Samii, A. (2012), "Dynamic analysis of concrete gravity dam-reservoir systems by Wavenumber approach in the frequency domain", *Earthq. Struct.*, **3**(3-4), 533-548.
Lotfi, V. and Zenz, G. (2017), "Time harmonic analysis of concrete gravity dam-reservoir systems by Wavenumber-TD approach", *J. Struct Eng Mech.*, Under Review.
Rabinovich, D., Givoli, D., Bielak, J. and Hagstrom, T. (2011), "A finite element scheme with a high order absorbing boundary condition for elastodynamics", *Comput. Meth. Appl. Mech.*, **200**(23-24), 2048-2066.
Samii, A. and Lotfi, V. (2012), "High-order adjustable boundary condition for absorbing evanescent modes of waveguides and its application in coupled fluid-structure analysis", *Wave Motion*, **49**(2), 238-257.
Sharan, S.K. (1987), "Time domain analysis of infinite fluid vibration", *Int. J. Numer. Meth. Eng.*, **24**(5), 945-958.
Sommerfeld, A. (1949), *Partial Differential Equations in Physics*, Academic Press, New York, U.S.A.
Tan, H. and Chopra, A.K. (1995), "Earthquake analysis of arch dam including dam-water-foundation rock interaction", *Earthq. Eng. Struct. Dyn.*, **24**(11), 1453-1474.
Waas, G. (1972), "Linear two-dimensional analysis of soil dynamics problems in semi-infinite layered media", Ph.D. Dissertation, University of California, Berkeley, California, U.S.A.
Zhen, Q., Minghui, L., Xiaodong, Z., Yao, Y., Cai, Z. and Jianyong, S. (2009), "The implementation of an improved NPML absorbing boundary condition in elastic wave modeling", *Appl. Geophys.*, **6**(2), 113-121.
Zienkiewicz, O.C., Taylor, R.L. and Zhu, J.Z. (2013), *The Finite Element Method*, Butterworth-Heinemann, Oxford, U.K.

AI